Assessment of Myocardial Perfusion with Multi-Detector Computed Tomography

G Coppini[1], R Favilla[1], B Barbagli[2], S Diciotti[2], S Lombardo[2], M Schlueter[1], L Salvatori[1], C Canapini[1], D Neglia[1], P Marraccini[1]

[1]CNR Institute of Clinical Physiology, Pisa, Italy
[2]Dept Electronics and Telecommunications, University of Florence, Florence, Italy

Abstract

A method to quantify the regional contrast enhancement as imaged during MDCT coronary angiography was developed. The procedure is based on the following steps: 1) Long axis reformatting and interactive selection of ventricular volume; 2) Normalization of image gray levels; 3) Extraction of the LV cavity by thresholding and blob growing; 4) LV segmentation by Fast Marching Level Set algorithm; 5) Building of bull-eye maps of the spatial distribution of contrast medium in the myocardium.

The method was tested on a dataset including the scans from 10 *patients with different perfusion defects. In* 5 *infarcted patients PET* $[^{13}N]$ *Ammonia scans were also performed: polar maps by CT imaging demonstrated well-defined regional perfusion defects consistent with PET imaging results.*

1. Introduction

Multi Detector Computed Tomography (MDCT) is employed in clinical practice mainly to image coronary arteries. On the other hand current MDCT systems allow the visualization of the entire heart volume during an entire heart cycle with high spatial and density resolution. MDCT imaging is thus opened to a wide spectrum of cardiac applications. As pointed out by other researchers [1], different pieces of information about coronary morphology, myocardium structure and function may be simultaneously collected leading to a more complete evaluation of the functional status of the heart.

In this report we focus on quantitative description of the spatial distribution of contrast medium in the myocardium that may provide valuable information about muscle perfusion and viability. In this view, a computational method to quantify the regional contrast enhancement as imaged during standard CT coronary angiography was developed.

2. Methods

To obtain quantitative descriptors of the opacified ventricular myocardium, the images acquired during MDCT coronary angiography must be properly calibrated. Moreover, in order to reliably process the resulting huge amount of images, automatic segmentation of LV wall is highly desirable.

2.1. Calibration

Gray levels of images acquired during the pass of contrast medium in the heart depend on the contribution of both muscle structures and contrast agent. For a given voxel at (x, y, z) in the myocardium we write the X-Ray attenuation coefficient as:

$$\mu(x, y, z) = \mu_{tissue}(x, y, z) + \alpha(x, y, z)\mu_{cm} \quad (1)$$

where $\mu_{tissue}(x, y, z)$ is the attenuation of preopacified tissue, $\alpha(x, y, z)$ is a space-varying coefficient accounting for the local amount of contrast agent with respect to a predefined value μ_{cm}. We assumed that the myocardium baseline attenuation μ_{tissue} is approximately constant and is estimated from a slice acquired before contrast agent injection. The value of μ_{cm} is computed as the average value in a RoI placed at the root of coronary arteries. Equation 1 can be solved with respect to α:

$$\alpha(x, y, z) = \frac{\mu(x, y, z) - \mu_{tissue}}{\mu_{cm}} \quad . \quad (2)$$

As the attenuation does not decrease after contrast agent injection and opacification is usually maximal at the coronary root, the following conditions are expected to be satisfied:

$$0 \leq \alpha(x, y, z) < 1 \quad \forall(x, y, z) \quad . \quad (3)$$

Therefore, the spatial distribution of $\alpha(x, y, z)$ is a normalized measure of myocardial opacification.

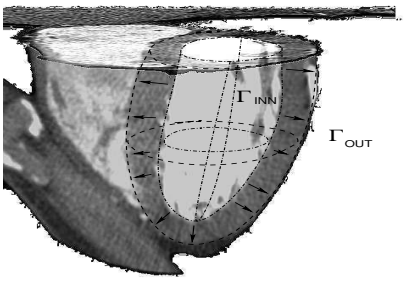

Figure 1. Finding the LV outer surface.

2.2. Segmentation

To build compact description of myocardial opacification, compatible with those employed in other imaging techniques, the following procedure to segment the LV wall volume was developed. As illustrated in figure 1, we based on the fact that the ventricular cavity, once filled with contrast medium, can be easily identified. Consequently, its external surface can be employed as the initial surface of a Fast Marching procedure [2] which is expected to evolve towards the outer boundary of the ventricle. The scheme of the procedure is illustrated in figure 2.

The heart volume is reformatted according to LV long axis by using standard software tools relying on user interaction. The Volume of Interest (VoI) including the LV from valvular plane to the apex is selected. To extract the cavity, a global threshold is estimated from gray level histogram. Afterwards standard blob growing is applied and the blob with the largest volume is retained as ventricular cavity. To cut papillary muscles away from the initial surface, the convex hull of LV cavity is computed on slice-by-slice basis.

Given the position of the inner boundary Γ_{INN} of LV wall, we may imagine it as evolving towards the outer surface Γ_{OUT} according to a given speed function $F(x, y, z) > 0$ that depends on the image gray levels. According to Fast Marching Level Set Methods this lead to the following non-linear Eikonal equation:

$$\begin{array}{c} F(x,y,z)||\nabla T|| = 1 \text{ in } R^3\ , \quad F(x,y,z) > 0 \\ T = 0 \ \text{ on } \ \Gamma_{INN} \end{array} \tag{4}$$

where $T(x, y, z)$ is the time at which the surface crosses the voxel at (x, y, z). Differently from general Level Sets methods, in Fast Marching one assumes that $F(x, y, z)$ is positive at each point (or, in general, it does not change sign). Thus the initial surface moves outwards only. This restriction implies a reduced computational load with respect to general Level Set methods. On the other hand, a monotonically evolving wavefront is well suited for LV wall shape.

1) Long axis reformatting of cardiac volume
2) Interactive selection of ventricular volume
3) Extraction of the LV cavity
4) Fast Marching Level Set algorithm

Figure 2. Phases of LV wall segmentation procedure.

A basic point to implement a correct fast marching segmentation is building an adequate velocity map from original CT values. To this end, we based on the fact that velocity should be *high* in correspondence of the myocardium in the left ventricle and should be *low* elsewhere so as to make the wavefront stop evolving near Γ_{OUT}. Though different choices are possible, we applied a Gaussian transformation $G_{\mu\sigma}$ to gray levels of opacified images. The average value μ being $150HU$ and the standard deviation σ $40HU$. Moreover to reduce the effect of statistical noise we applied to each slice an anisotropic diffusion filter (conductance 2, iteration number 10, time step 0.0625) [3]. Some examples of segmentations are shown in figure 3.

Once the LV wall is extracted from the CT scan, the values of $\alpha(x, y, z)$ are computed according to equation 2 and utilized to build a bi-dimensional polar map representation (bull-eye) of the spatial distribution of contrast agent. We adopted the standard 17 segments bull-eye [4] used also in PET and SPECT imaging.

3. Experiments

The potential of the method was tested on a clinical dataset of MDCT scans.

3.1. Patients

Ten patients (65 ± 3 years old) with suspected or proved coronary artery disease underwent diagnostic MDCT coronary angiography for risk stratification or follow-up program. Out of these subjects, five underwent perfusion PET scanning with $[^{13}N]$ Ammonia [5].

3.2. Imaging

MDCT examinations were performed using a GE LightSpeed 64 VCT scanner. Patients were pretreated with proponolol (2 mg i.v.) and isorbide denitrate (0.6 mg i.v.) as clinically indicated. After the scout of the thorax an axial slice with voxel size $0.625 \times 0.625 \times 2.5$ mm was obtained before contrast medium injection. This slice was used for calibration. A non-ionic iodinated contrast agent (IOMERON 400, Bracco Imaging Italia s.r.l.) was injected (infusion rate equal or greater than 5 ml/s), the total volume of contrast ranging from 80 to 120 ml. Acquisition

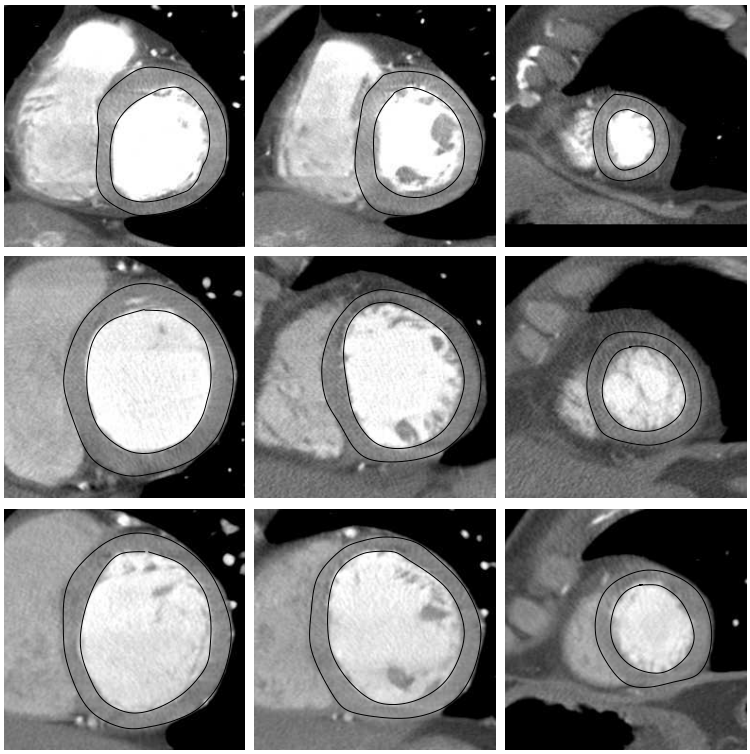

Figure 3. Examples of LV segmentation in three different patients (top to bottom). For each patient one basal, one mid and one apical slice are shown from left to right.

LV Region	S	E_+	E_-
Basal	96.2 ± 3.9	4.1 ± 4.2	3.1 ± 3.8
Mid	97.1 ± 4.2	3.1 ± 4.0	4.1 ± 3.5
Apical	91.1 ± 4.3	8.2 ± 4.1	4.2 ± 3.9
Total	94.8 ± 3.4	5.1 ± 2.7	3.8 ± 0.7

Table 1. LV Segmentation results.

time was optimized by a bolus tracking monitoring system. Volume raw data were acquired using an ECG-gating technique: ECG-gated phases were retrospectively reconstructed using intervals of 10% of R-R period and a voxel size of $0.625 \times 0.625 \times 0.6$ mm.

PET scans were performed using a GE Discovery CT/PET. Patient positioning was confirmed by scout view. In addition, a transmission scan for attenuation correction was performed. Thereafter 370 MBeq $[^{13}N]$ ammonia were injected i.v., at the same time dynamic PET acquisition was started. At least after 45 minutes (the decay time of $[^{13}N]$ ammonia activity) dipyridamole (0.56 mg/kg) was injected i.v. over 4 minutes. A second dose of 370 MBeq $[^{13}N]$ ammonia was injected five minutes after the end of dipyridamole infusion, at the same time a second scan of dynamic PET acquisition was started. Tomographic reconstruction of myocardial images was obtained in short, long and vertical axes. The computation of myocardial blood flow was done according to monocompartment modeling.

4. Results

First of all, the quality of obtained segmentations was evaluated. In all the cases, expert observers confirmed that segmentations were anatomically correct with no artifact. In addition, manual segmentations by an experienced observer were compared with the computed ones. For each patient, the observer was asked to select three slices (one at ventricle base, the second in the mid region and the third in the apical region) and manually delineate the LV wall. For each slice, let R_o the region drawn by the observer and R_c the computed one. We computed the number N_{TP} of voxels belonging to R_o and R_c simultaneously, the number N_+ of voxels belonging to R_c but not in R_o, and the number N_- of voxels belonging to R_o but not in R_c. These quantities were normalized by the number of voxels N_o in R_o:

$$S = \frac{N_{TP}}{N_o} \ , \ E_+ = \frac{N_+}{N_o} \ , \ E_- = \frac{N_-}{N_o} \quad . \qquad (5)$$

In this way, S measures the sensitivity of the segmentation, E_+ represents the overestimation error and E_- the

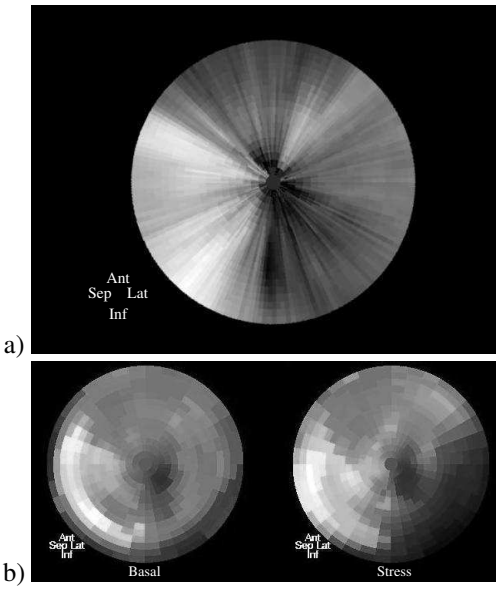

Figure 4. a) bull-eye diagram from MDCT opacification at diastole, b) bull-eye diagram (both basal and stress) of perfusion PET.

underestimation error. For each of the three ventricular regions, in table 1 we provide the (percentage) values of S, E_+, E_- averaged over the dataset. Segmentation of the apical region exhibits inferior sensitivity with a higher over-estimation error as compared both to basal and mid regions. This is probably due to partial volume effect. As shown in the bottom raw of table 1, on the average sensitivity was about $94.8 \pm 4.1\%$, with $E_+ = 5.1 \pm 4.1$ and $E_- = 3.8 \pm 3.7$.

Finally, MDCT bull-eye diagrams were visually compared with PET perfusion diagrams. According to the judgment of experienced observers, well defined regional perfusion defects are consistently represented in both diagrams. In figure 4a) an example of MDCT bull-eye map is shown along with PET $[^{13}N]$ ammonia bull-eye diagram (basal and stress) in panel b). This clinical example shows how MDCT opacification maps are able to describe the blood flow distribution in the myocardium in a manner similar to PET perfusion maps. In particular, in this patient MDCT correctly indicates the presence of severe perfusion defects in apical and infero-lateral segments and a moderate perfusion defect in anterior segments.

5. Discussion and conclusions

Quantitative description of regional opacification of LV myocardium, as imaged in MDCT coronary angiography, has been investigated leading to the development of a dedicated computational procedure. The method was tested on a clinical dataset including 10 patients undergoing MDCT coronary angiography.

At present, the calibration phase is based on the simplified assumption that myocardial attenuation does not depend on spatial coordinates (x, y, z). It is worth nothing that, in many cases, spatial changes of μ_{tissue} are quite limited with respect to the contribution of contrast agent so that small calibration errors are expected to occur. Anyway, a space-varying calibration procedure is currently under investigation. As to the segmentation procedure, we obtained good sensitivity with reasonable over- and under-estimation errors.

It must be pointed out that other possible sources of error are related to the inherent limits of current MDCT technology. In particular, scans employ several heart cycles with possible blurring and, more in general, motion artifacts. It is reasonable that the evolution of MDCT technology that is now leading to very reduced imaging times will result in noticeable image quality improvements.

The reader should notice that MDCT bull-eye maps obtained from calibrated scans provide compact descriptions of the spatial distribution of contrast agent. Their use is expected to ease the investigation of the relationship among coronary vessels and perfused territories. Furthermore qualitative comparison of MDCT opacification maps with PET ammonia perfusion map support the idea that perfusion defects may be detected also by MDCT imaging. This findings prompted us to undertake further investigations utilizing an extended dataset.

References

[1] Mahnken, AH and Mühlenbruch, G and Günter, GW and Wildberger, JE. Cardiac CT: coronary arteries and beyond. European Radiology 2007;17:9941008.

[2] Sethian, JA. A Fast Marching Level Set Method for Monotonically Advancing Fronts. Proc Natl Acad Sci 1996; 93:1591–1595.

[3] Perona, P and Malik, J. Scale-Space and Edge Detection using Anisotropic Diffusion. IEEE Trans Pattern Anal and Machine Intell 1990;12:629–639.

[4] Cerqueira, MD and Weissman, NJ and Dilsizian, V and Jacobs, AK and Kaul, S and Laskey, WK and Pennell, DJ and Rumberger, JA and Ryan, T and Verani, MS. Standardized myocardial segmentation and nomenclature for tomographic imaging of the heart. Circulation 2002;105:539–542.

[5] Neglia, D and Rimoldi, O and Kaufmann, PA and Camici PG. Radionuclide PET and PET/CT in coronary artery disease. Curr Pharm Des 2008;14:1798–1814.

Address for correspondence:

Giuseppe Coppini
CNR Institute of Clinical Physiology,
Via Moruzzi, 1 56124 Pisa, Italy
coppini@ifc.cnr.it